

Numerical Simulation of High Mach Number Flow using the Finite Difference Lattice Boltzmann Method (FDLBM)

Seyedabbas Sadatsakak*

Imam Khomeini international university, Qazvin, Iran; sakak@ENG.ikiu.ac.ir

Abstract

The Lattice Boltzmann Method (LBM) is known as a powerful numerical tool to simulate fluid flow problems. Particularly, it has shown a unified strength for solving incompressible fluid flows in complicated geometries. Many researchers have used Lattice Boltzmann (LB) concept to simulate compressible flows, but the common defect of most of previous models is the stability problem at high Mach number fluid flows. In this paper we introduce a FLDBM-model, which is capable to simulate fluid flows with any specific heat ratios and higher Mach numbers, from 0 to 30 or higher. Compressibility is applied using multiple particle speeds in a thermal fluid. Based on the discrete-velocity-model, a new finite difference method and an artificial viscosity are implemented, which must find a balance between numerical stability and accuracy of simulation. The introduced model is checked and validated against well-known benchmark tests such as one dimensional shock tubes, supersonic bump and ramp (two dimensional). Both sets of results have a reasonable agreement regarding to exact solutions.

Keywords: Finite Difference, High Mach Number Flow, Lattice Boltzmann Method

1. Introduction

Recently the Lattice Boltzmann (LB) method has been successfully applied to simulate processes in complex physical systems, especially in case of incompressible fluids flow simulation¹. This method is very powerful in simulation of high-speed compressible flows². The LB method has shown its strength in simulation of many fields such as hydrodynamics, multiphase and multi-component fluid flows and much more complex situations³. Although the LB method has shown its fantastic abilities to simulate fluid flows in complex composition systems, it has some limits to consider as a general computational tool. One of them is the low Mach number constraint.

The multispeed thermal model is often used to present heat capacity ratios and compressibility of fluids^{4,5}.⁶ has introduced the solving the LBM under considering the finite difference method (FDLBM). The FDLBM has some strength against the LBM. First of all, the FDLBM can improve numerical stability by selecting a suitable

time step. Secondly, it uses a generalized coordinate system which can be fitted to the shape of the boundary. Simulation of the compressible Navier–Stokes system including contact discontinuities is a challenging work^{7–14}.

2. Finite difference lattice Boltzmann method

The Finite-Difference Lattice Boltzmann (FDLB) is used, which enables us to consider conservation equations of mass, momentum and energy of a fluid flow¹⁵.

The distribution function f_{ki} with the Bhatnager–Gross–Krook approximation²⁴ can be written as,

$$\frac{\partial f_{ki}}{\partial t} + c_{ki\alpha} \frac{\partial f_{ki}}{\partial r_{\alpha}} = -\frac{1}{\tau} (f_{ki} - f_{ki}^{(0)}) \quad (1)$$

The local density ρ , the hydrodynamic velocity \mathbf{u}_{α} , and the translational internal energy \mathbf{e} can be approximated as:

*Author for correspondence

$$\rho = \sum_{ki} f_{ki} \quad (2)$$

$$\rho u_\alpha = \sum_{ki} f_{ki} c_{ki\alpha} \quad (3)$$

$$\rho \left(\frac{D+n}{D} e + \frac{u^2}{2} \right) = \sum_{ki} f_{ki} \left(\frac{c_k^2}{2} + \frac{\eta_k^2}{2} \right) \quad (4)$$

Applying the Chapman expansion:

$$\frac{\partial \rho}{\partial t} + \frac{\partial(\rho u_\alpha)}{\partial r_\beta} = 0$$

$$\frac{\partial(\rho u_\alpha)}{\partial t} + \frac{\partial}{\partial r_\beta} (\rho u_\alpha u_\beta + P \delta_{\alpha\beta}) - \frac{\partial}{\partial r_\beta} \left[\mu \left(\frac{\partial u_\beta}{\partial r_\alpha} + \frac{\partial u_\alpha}{\partial r_\beta} - \frac{2}{D+n} \frac{\partial u_\gamma}{\partial r_\gamma} \delta_{\alpha\beta} \right) \right] = 0 \quad (5)$$

$$\frac{\partial}{\partial t} \left[\rho \left(E + \frac{u^2}{2} \right) \right] + \frac{\partial}{\partial r_\alpha} \left[\rho u_\alpha \left(E + \frac{u^2}{2} + \frac{P}{\rho} \right) \right] - \frac{\partial}{\partial r_\alpha} \left[\kappa' \frac{\partial e}{\partial r_\alpha} + \mu u_\beta \left(\frac{\partial u_\beta}{\partial r_\alpha} + \frac{\partial u_\alpha}{\partial r_\beta} - \frac{2}{D+n} \frac{\partial u_\gamma}{\partial r_\gamma} \delta_{\alpha\beta} \right) \right] = 0$$

Viscosity coefficient μ and heat conductivity κ' and pressure P are defined as:

$$P = \frac{2}{D} \rho e$$

$$\mu = \frac{2}{D} \rho e \tau \quad (6)$$

$$\kappa' = \frac{2(D+n+2)}{D(D+n)} \rho e \tau$$

E is the sum of the energies,

$$E = \frac{D+n}{D} e \quad (7)$$

The specific heat ratio γ , is defined as

$$T = \frac{2}{D} e$$

$$\gamma = \frac{D+n+2}{D+n} \quad (8)$$

$$\alpha = \sqrt{\gamma T}$$

The equilibrium distribution function f_{ki}^{eq} is derived as a function of flow velocities from the Maxwellian functions:

$$f^{eq} = \frac{\rho}{2\pi e} \exp \left[-\frac{1}{2e} (c_{ki\xi} - u_\xi)^2 \right] = \frac{\rho}{2\pi e} \exp \left(-\frac{1}{2e} c_k^2 \right) \exp \left[\frac{1}{e} (c_{ki\xi} u_\xi - \frac{u^2}{2}) \right] \quad (9)$$

To consider Navier–Stokes equations, equilibrium distribution function should be presented as follows:

$f_{ki}^{eq} = \frac{\rho}{2\pi e} \exp \left[-\frac{1}{2e} (c_{ki\xi} - u_\xi)^2 \right] = \frac{\rho}{2\pi e} \exp \left(-\frac{1}{2e} c_k^2 \right) \exp \left[\frac{1}{e} (c_{ki\xi} u_\xi - \frac{u^2}{2}) \right]$

where, the parameter F_k is a function of e and c_k . F_k is calculated as:

$$F_0 = 1 - 8(F_1 + F_2 + F_3 + F_4 + F_5 + F_6 + F_7 + F_8) \quad (11)$$

$$F_1 = \frac{n}{\eta_1^2} \frac{6e^4 - (c_2^2 + c_3^2 + c_4^2)e^3 + \frac{1}{4}(c_2^2 c_3^2 + c_2^2 c_4^2 + c_3^2 c_4^2)e^2 - \frac{1}{8}c_2^2 c_3^2 c_4^2 e}{(c_1^2 - c_2^2)(c_1^2 - c_3^2)(c_1^2 - c_4^2)}$$

$$F_2 = \frac{n}{\eta_2^2} \frac{6e^4 - (c_3^2 + c_4^2 + c_1^2)e^3 + \frac{1}{4}(c_3^2 c_4^2 + c_3^2 c_1^2 + c_4^2 c_1^2)e^2 - \frac{1}{8}c_3^2 c_4^2 c_1^2 e}{(c_2^2 - c_3^2)(c_2^2 - c_4^2)(c_2^2 - c_1^2)}$$

$$F_3 = \frac{n}{\eta_3^2} \frac{6e^4 - (c_4^2 + c_1^2 + c_2^2)e^3 + \frac{1}{4}(c_4^2 c_1^2 + c_4^2 c_2^2 + c_1^2 c_2^2)e^2 - \frac{1}{8}c_4^2 c_1^2 c_2^2 e}{(c_3^2 - c_4^2)(c_3^2 - c_1^2)(c_3^2 - c_2^2)}$$

$$F_4 = \frac{n}{\eta_4^2} \frac{6e^4 - (c_1^2 + c_2^2 + c_3^2)e^3 + \frac{1}{4}(c_1^2 c_2^2 + c_1^2 c_3^2 + c_2^2 c_3^2)e^2 - \frac{1}{8}c_1^2 c_2^2 c_3^2 e}{(c_4^2 - c_1^2)(c_4^2 - c_2^2)(c_4^2 - c_3^2)}$$

$$F_5 = -F_1 + \frac{48e^4 - 6(c_2^2 + c_3^2 + c_4^2)e^3 + (c_2^2 c_3^2 + c_3^2 c_4^2 + c_4^2 c_2^2)e^2 - \frac{1}{4}c_2^2 c_3^2 c_4^2 e}{c_1^2(c_1^2 - c_2^2)(c_1^2 - c_3^2)(c_1^2 - c_4^2)}$$

$$F_6 = -F_2 + \frac{48e^4 - 6(c_3^2 + c_4^2 + c_1^2)e^3 + (c_3^2 c_4^2 + c_4^2 c_1^2 + c_1^2 c_3^2)e^2 - \frac{1}{4}c_3^2 c_4^2 c_1^2 e}{c_2^2(c_2^2 - c_3^2)(c_2^2 - c_4^2)(c_2^2 - c_1^2)}$$

$$F_7 = -F_3 + \frac{48e^4 - 6(c_4^2 + c_1^2 + c_2^2)e^3 + (c_4^2 c_1^2 + c_1^2 c_2^2 + c_2^2 c_4^2)e^2 - \frac{1}{4}c_4^2 c_1^2 c_2^2 e}{c_3^2(c_3^2 - c_4^2)(c_3^2 - c_1^2)(c_3^2 - c_2^2)}$$

$$F_8 = -F_4 + \frac{48e^4 - 6(c_1^2 + c_2^2 + c_3^2)e^3 + (c_1^2 c_2^2 + c_2^2 c_3^2 + c_3^2 c_1^2)e^2 - \frac{1}{4}c_1^2 c_2^2 c_3^2 e}{c_4^2(c_4^2 - c_1^2)(c_4^2 - c_2^2)(c_4^2 - c_3^2)}$$

And the groups of particle velocities are selected as following:

$$(c_1, c_2, c_3, c_4, c_5, c_6, c_7, c_8) = (1, 2, 3, 4, 1, 2, 3, 4)$$

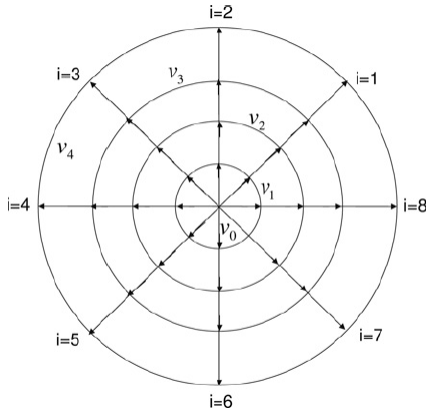
$$(\eta_1, \eta_2, \eta_3, \eta_4, \eta_5, \eta_6, \eta_7, \eta_8) = (1, 2, 3, 4, 0, 0, 0, 0) \quad (12)$$

Table 1. Particle velocities

η_k	c_k	i : direction	k : group
0	0	1	0
η_1	c_1	1~8	1
η_2	c_2	1~8	2
η_3	c_3	1~8	3
η_4	c_4	1~8	4
0	$c_5 = c_1$	1~8	5
0	$c_6 = c_2$	1~8	6
0	$c_7 = c_3$	1~8	7
0	$c_8 = c_4$	1~8	8

3. Artificial Viscosity and Modified Lax-Wendroff Scheme

The original LW scheme is not suitable to model capture shocks. Therefore, an artificial viscosity is added to Eq. (1):



We use non-dimensionalized according to the Table 1.

Table 2. Non-dimensional form of macroscopic and microscopic variables

Parameter type	Parameter name	Reference Term
Density	$\rho, f_{ki}, f_{ki}^{eq}$	ρ_0
Velocity	$c_{ki\alpha}, u_\alpha$	$\sqrt{RT_0}$
Energy	e, E	RT_0
Temperature	T	T_0
Coordinate	r_α	L
Time	t, τ	$\frac{L}{\sqrt{RT_0}}$
Pressure	P	$\rho_0 RT_0$
Diffusion	μ, κ'	$\rho_0 L \sqrt{RT_0}$

In Table 1, ρ_0, L and T_0 are Reference variables and R is gas constant.

$$\frac{\partial f_{ki}}{\partial t} + c_{ki\alpha} \frac{\partial f_{ki}}{\partial r_\alpha} = -\frac{1}{\tau} (f_{ki} - f_{ki}^{(0)}) + \frac{c_{ki\alpha}(1 - v_{ki\alpha}^2)\Delta r_\alpha^2}{6} \frac{\partial^3 f_{ki}}{\partial r_\alpha^3} + \theta_{\alpha l} |k_\alpha| \frac{(1 - |k_\alpha|)(\Delta r_\alpha^2)}{2\Delta t} \frac{\partial^2 f_{ki}}{\partial r_\alpha^2}$$

$$v_{ki\alpha} = c_{ki\alpha} \frac{\Delta t}{\Delta r_\alpha}$$

$$k_\alpha = u_\alpha \frac{\Delta t}{\Delta r_\alpha}$$

$$\theta_{\alpha l} = \lambda \left| \frac{P_{\alpha l+1} - 2P_{\alpha l} + P_{\alpha l-1}}{P_{\alpha l+1} + 2P_{\alpha l} + P_{\alpha l-1}} \right|$$

λ is used to control the viscosity. We use the LW and central difference for Eq. (13):

$$f_{kil}^{new} = f_{kil} - \frac{v_{ki\alpha}}{2} (f_{kil+1} - f_{kil-1}) - \frac{\Delta t}{\tau} (f_{kil} - f_{kil}^{eq}) + \frac{v_{ki\alpha}^2}{2} (f_{kil+1} - 2f_{kil} + f_{kil-1}) + \frac{v_{ki\alpha}(1 - v_{ki\alpha}^2)}{12} (f_{kil+2} - 2f_{kil+1} + 2f_{kil-1} - f_{kil-2}) + \frac{\theta_{\alpha l} |k_\alpha| (1 - |k_\alpha|)}{2} (f_{kil+1} - 2f_{kil} + f_{kil-1})$$

4. Tests and analysis

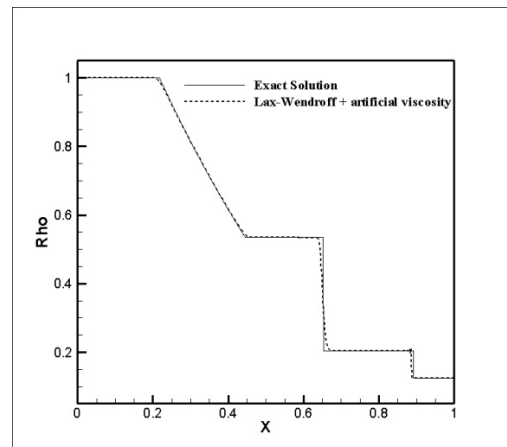
One dimensional Riemann problem and two dimensional supersonic Ramp and bump are used to show the accuracy and performance of new model.

4.1 First Test Case: One Dimensional Riemann Problem

This problem is a well-known Riemann problem presented by Sod. In the Sod problem, there is:

$$\begin{cases} (\rho, u_1, u_2, T)|_{\mathbb{R}_L} = (1, 0, 0, 1) \\ (\rho, u_1, u_2, T)|_{\mathbb{R}_R} = (0.125, 0, 0, 0.8) \end{cases}$$

The agreements of different parameters are shown in Figure 1.



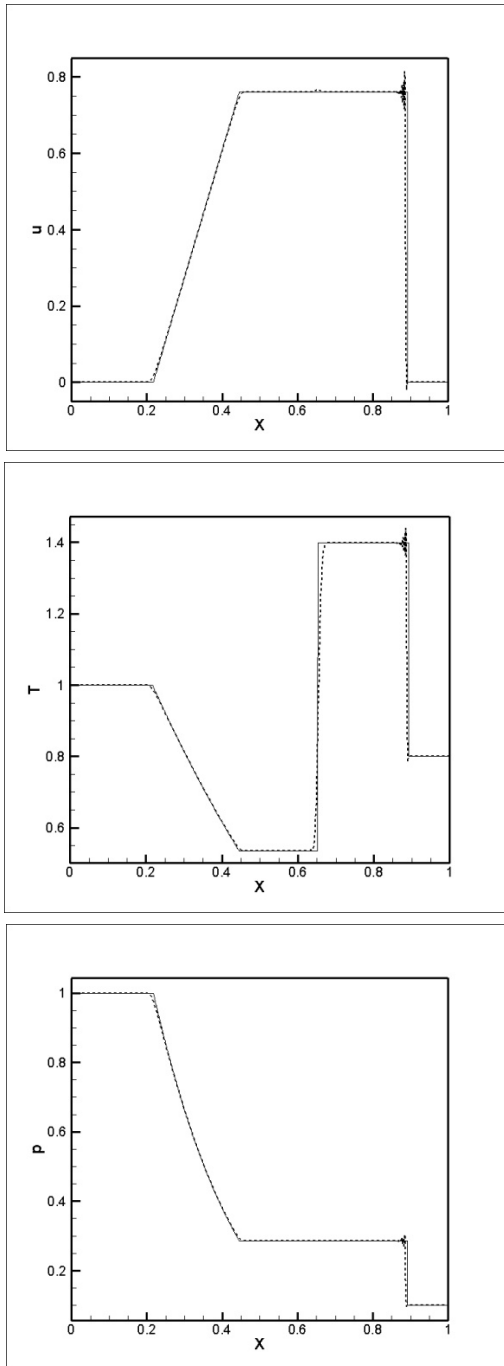


Figure 1. Sod shock tube.

4.2 Second Test Case

Second test case is the supersonic ramp with an inlet Mach number of 2.0. The geometry includes a $10^\circ 10^\circ$ compression ramp with an 10° expansion corner. Figure 2 shows the generated grid for supersonic ramp. Figure 3 shows the computed pressure coefficient at lower wall and compare it with exact solution, which shows satis-

fyng agreement. Figure 4 shows the contours of Mach, Density, Internal Energy and Pressure at steady state. Figure 5 shows the contour of Mach number at different time steps.

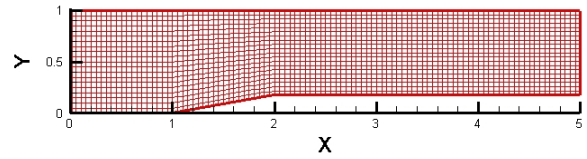


Figure 2. Computational domain for supersonic ramp.

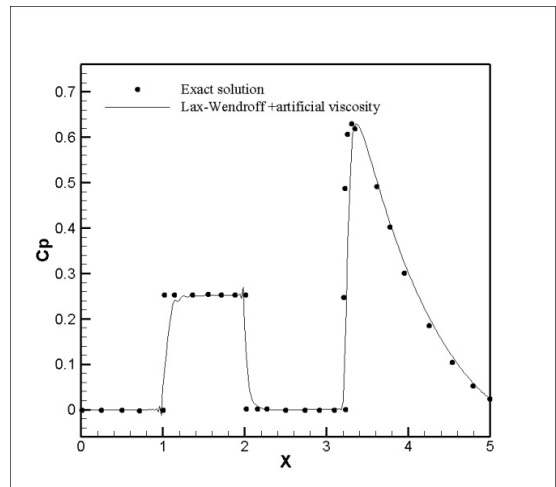
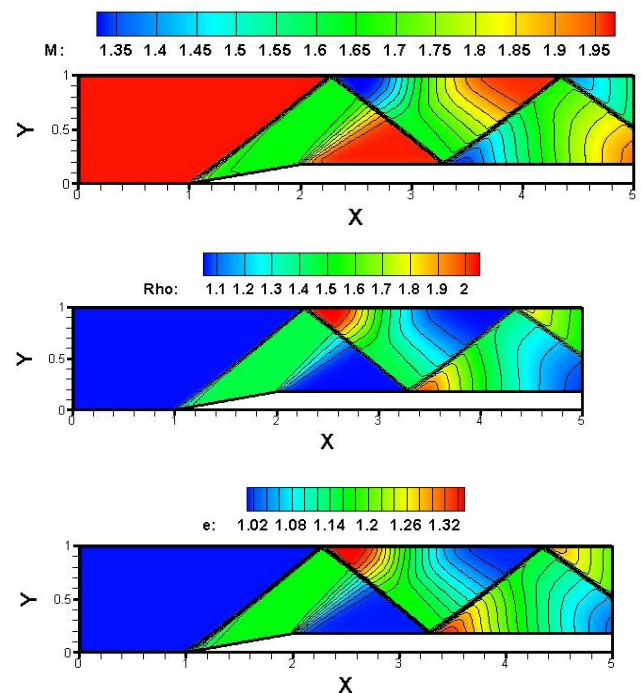


Figure 3. Comparison of numerical and theoretical Cp for supersonic test case.



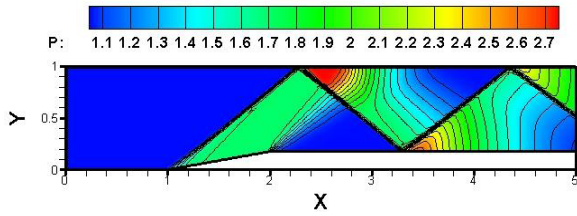


Figure 4. Contours of Mach, Density, Internal Energy and Pressure at steady state.

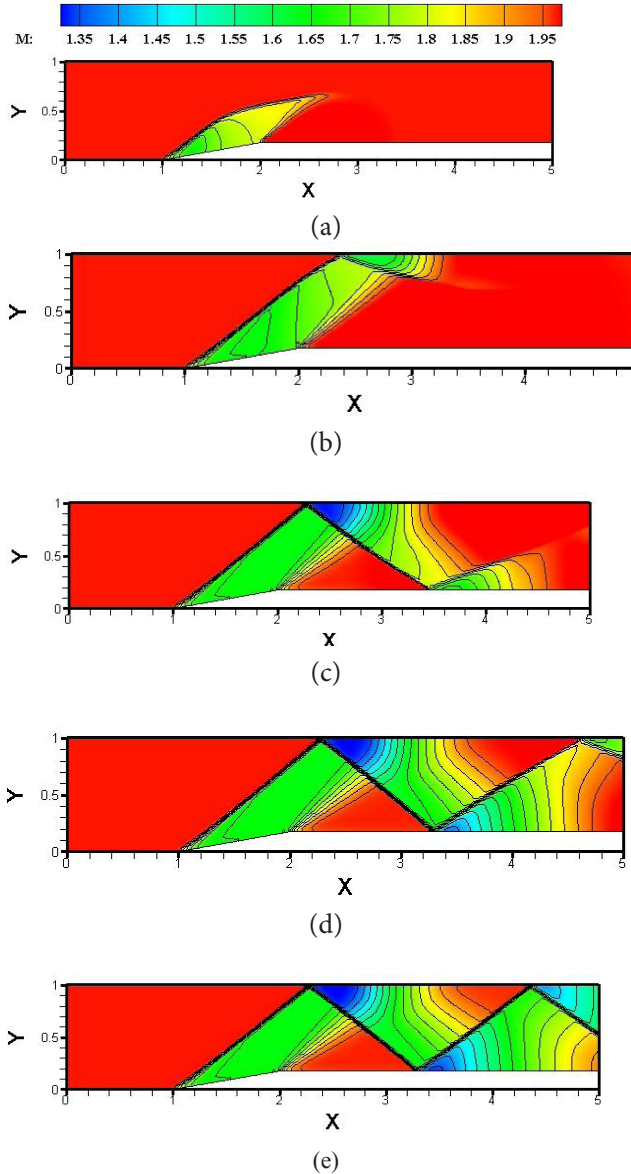


Figure 5. Contours of Mach number at different time steps.

4.3 Third Test Case

Figure 6 shows the generated grid for supersonic bump. Figures 7 and 8 show the computed mach number at

lower and upper walls, which shows a good agreement. Figure 9 shows the contours of Mach, Density, Internal Energy and Pressure at steady state. Figure 10 shows the contour of Mach number at different time steps.

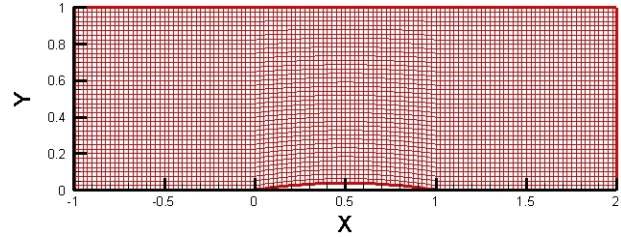


Figure 6. Computational domain for supersonic bump.

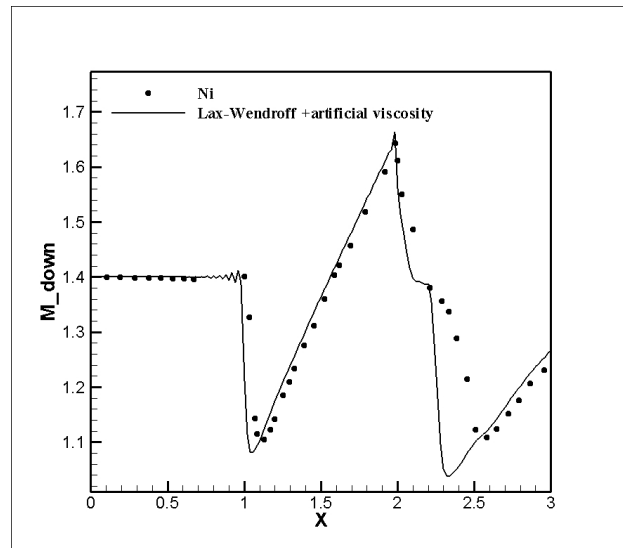


Figure 7. Mach number on lower wall.

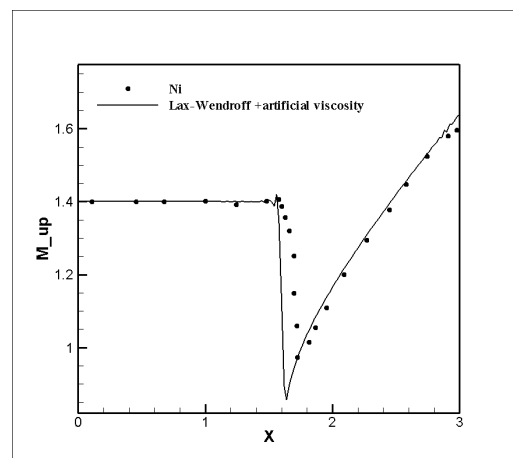


Figure 8. Mach number on upper wall.

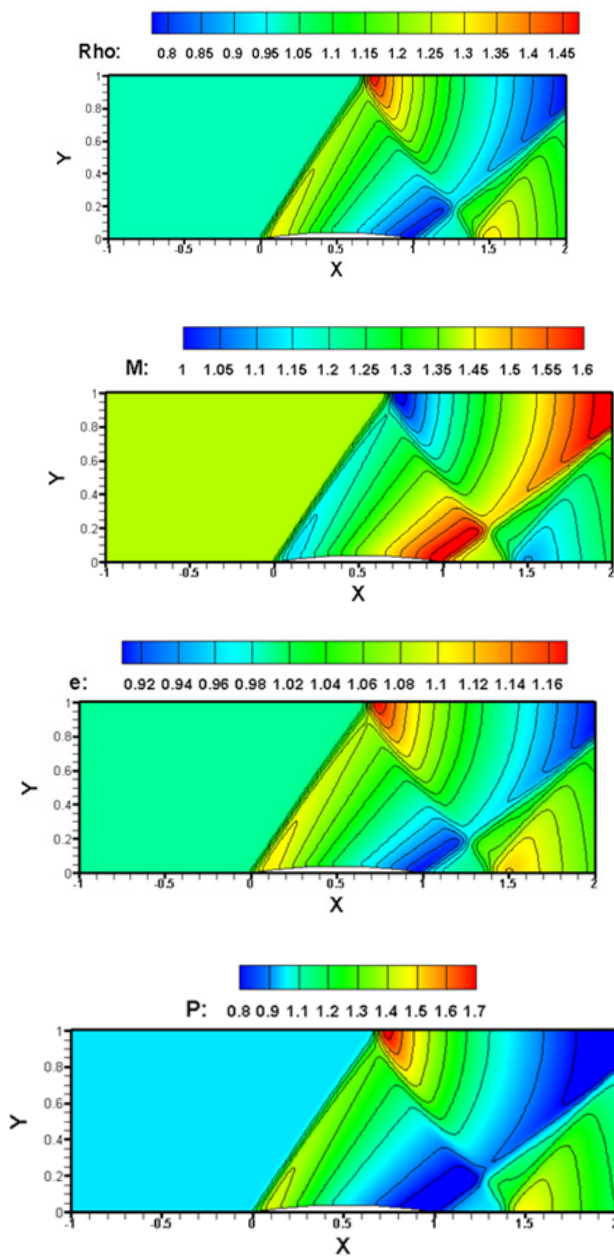


Figure 9. Contours of mach, density, internal energy and pressure at steady state.

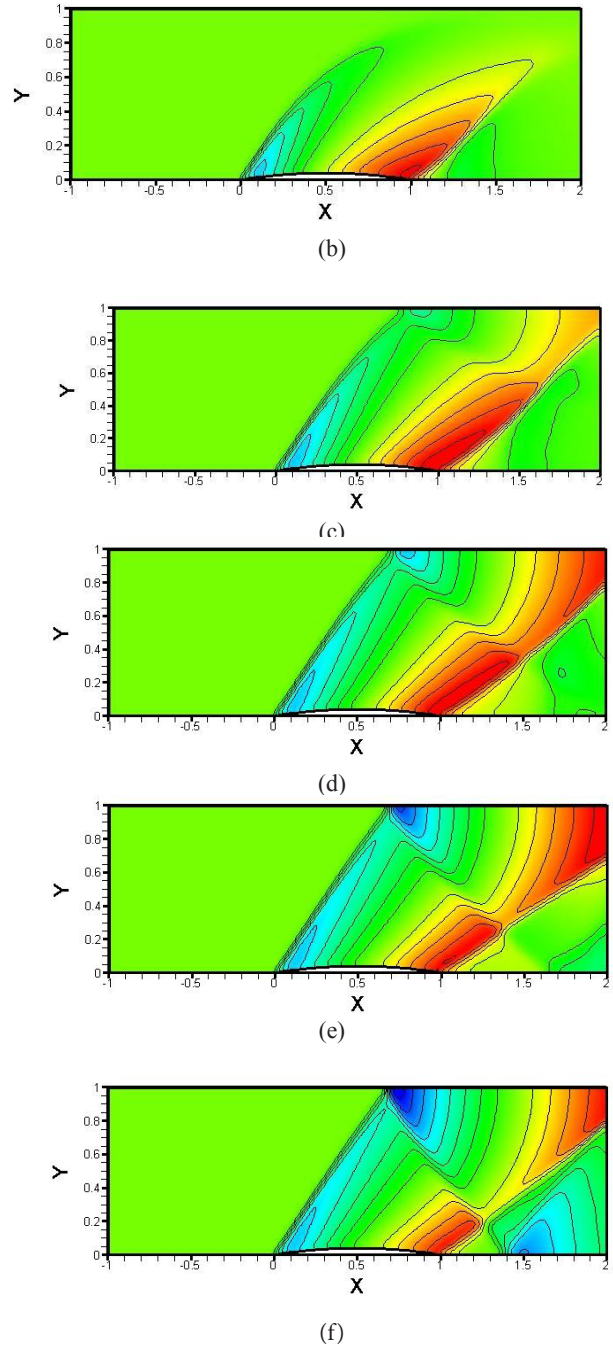
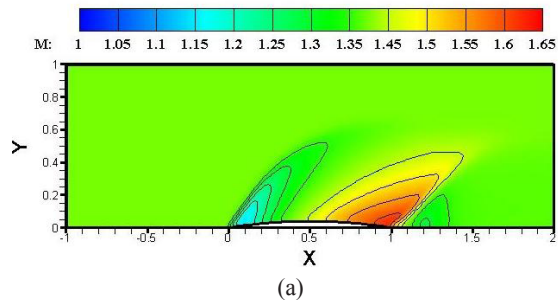


Figure 10. Contours of mach number at different time steps.

5. Conclusions

Lattice Boltzmann model for compressible flows is used frequently. Although low Mach number flows show good results regarding to exact solutions, the high Mach number flows shows difficulties in stabilities criterion, because von Neumann stability condition stays unsatisfied. The presented model tries to overcome this problem

with composing DVM-method by Watari, an improved Lax–Wendroff scheme and using an additional fictitious viscosity. Some typical tests are introduced to check presented model, which shows good agreement and stability.

The model also shows the very good accuracy in two dimensional problems (Supersonic Bump and Ramp), in both steady and unsteady cases.

Future work should concentrate on the stability versus accuracy of introduced method.

6. References

1. Succi S. The Lattice Boltzmann equation for fluid dynamics and beyond, Oxford University Press, New York; 2001.
2. Xu AG, Pan XF, Zhang GC, Zhu JS. *J. Phys.: Condens. Matter* 19 (2007) 326212.
3. Wu QF, Chen WF. DSMC method for heat chemical non-equilibrium flow of high temperature rarefied gas. National Defence Science and Technology University Press, Beijing; 1999.
4. McNamara G, Alder B. *Physica A* 194 (1993) 218.
5. Alexander FJ, Chen S, Sterling JD. *Phys. Rev. E* 47 (1993) R2249.
6. Cao N, Chen S, Jin S, Martinez D. *Phys. Rev. E* 55 (1997) R21.
7. Yan G, Chen Y, Hu S. *Phys. Rev. E* 59 (1999) 454.
8. Yu H, Zhao K. *Phys. Rev. E* 61 (2000) 3867.
9. Sun C. *Phys. Rev. E* 58 (1998) 7283.
10. Sun C. *Phys. Rev. E* 61 (2000) 2645.
11. Sun C, Hsu AT. *Phys. Rev. E* 68 (2003) 016303.
12. Kataoka T, Tsutahara M. *Phys. Rev. E* 69 (2004) 035701(R); *Phys. Rev. E* 69 (2004) 056702.
13. Watari M, Tsutahara M. *Phys. Rev. E* 67 (2003) 036306; *Phys. Rev. E* 70 (2004) 016703.
14. Xu AG, *Europhys. Lett.* 69 (2005) 214; *Phys. Rev. E* 71 (2005) 066706; *Prog. Theor. Phys. (Suppl.)* 162 (2006) 197.
15. Watari M, Tsutahara M. *Phys. Rev. E* 67 (2003) 036306; *Phys. Rev. E* 70 (2004) 016703.
16. Xu A. *Europhys. Lett.* 69 (2005) 214; *Phys. Rev. E* 71 (2005) 066706; *Prog. Theor. Phys. (Suppl.)* 162 (2006) 197.